

## Detection of Three Perennial Crops with Two Supervised Classification Methods from Landsat-8 and Sentinel-2 Satellite Images

Lidia Vlassova<sup>1</sup>, Elian Briohildo Intriago Giler<sup>2</sup>, Betty Beatriz González Osorio<sup>3</sup>, Byron Wladimir Oviedo Bayas<sup>4</sup>, Olga A. Rosero-Vlasova<sup>5</sup>

### Abstract

*In order for there to be adequate territorial planning, an orderly occupation of the territory is necessary; The main input is reliable information on land cover. Therefore, in recent times, new remote sensing methods have been born that need to be tested. This research compared the accuracy of the traditional remote sensing method, Maximum Likelihood (ML), versus an artificial intelligence-based method called Random Forest (RF), in the detection of banana, cocoa and palm crops (in addition to other covers). Satellite imagery from Landsat-8 and Sentinel-2 was used, which was downloaded from the USGS website; the bands in the Sentinel-2 image were atmospheric correction applied with QGIS plugins created by Congedo (2021). For the two images, the spectral indices NDVI, GNDVI, GCI and MSI were calculated, and the regions of interest (ROIs) were created on the stack of calculated indices of each image; For the creation of ROIs (both for training and validation of results) coordinates were taken in situ and from Google Earth Pro version 7.3.4.8642. ML classification was performed in ENVI 5.3 software and RF classification was performed in QGIS 3.22.7 with Dzetsaka tools created by (Karasiak, 2019). For the validation of results, the traditional confusion matrix and the Kappa coefficient proposed by Cohen (1960). The results showed that RF is slightly superior to ML, although with certain nuances. In general, the classification of Sentinel-2 with RF obtained better accuracy (89%), although for the detection of the aforementioned crops it was the least accurate.*

**Keywords:** *Maximum Likelihood, Random Forest, spectral indices, land cover.*

### 1. Introduction

Ecuador is a country with a large number of agricultural crops that allow it to supply part of the national and international market (Salmoral et al., 2018); These crops include bananas (*Musa × paradisiaca*), cocoa (*Theobroma cacao*) and African palm (*Elaeis guineensis*). These agricultural activities provide numerous economic and social benefits that improve the quality of life of the population (Gama-Rodrigues et al., 2021; Osvaldo

---

<sup>1</sup> PhD in Geography and Territory Planning. Quevedo State Technical University Quevedo-Ecuador, lvlasova@uteq.edu.ec, <https://orcid.org/0000-0001-5025-5691>

<sup>2</sup> Ing. Ambiental. Universidad Técnica Estatal de Quevedo. Quevedo, Ecuador, elian.intriago2017@uteq.edu.ec, [Orcid.org/0000-0002-6018-4302](https://orcid.org/0000-0002-6018-4302)

<sup>3</sup> PhD in Economics of Natural Resources and Sustainable Development, specializing in Environmental Economics. Quevedo State Technical University Quevedo-Ecuador, bgonzález@uteq.edu.ec, [http://orcid.org/0000-0002-2851-2660](https://orcid.org/0000-0002-2851-2660)

<sup>4</sup> PhD en Tecnologías de la Información y Comunicación, Quevedo State Technical University Quevedo-Ecuador, boviedo@uteq.edu.ec, [http://orcid.org/0000-0002-5366-5917](https://orcid.org/0000-0002-5366-5917)

<sup>5</sup> Universidad de Fuerzas Armadas ESPE, Km. 24 vía Santo Domingo – Quevedo, Hda. Zoila Luz, Avenida Quevedo 3-703-914, Santo Domingo 230153, Ecuador

Bardomiano, 2014; Sánchez Castañeda, 2017). According to the Agricultural Public Information System (SIPA), between 2010-2021 the average annual harvested area of banana, cocoa and palm crops in the country was 181570.83 ha, 449622.92 ha and 219265.17 ha, respectively; In the same period, banana, cocoa (dried almond) and palm crops produced an annual average of 6742078.75 t, 225741.08 t and 2800278.667 t, with average annual yields of  $37.28 \text{ t}\cdot\text{ha}^{-1}$ ,  $0.49 \text{ t}\cdot\text{ha}^{-1}$  and  $12.83 \text{ t}\cdot\text{ha}^{-1}$ , in the same order (SIPA, 2021). In addition, the province of Los Ríos is part of the group of three provinces in which 70% is produced at the national level (MCPEC et al., 2014).

From the above figures, it is evident that agriculture plays an important role in the economic and social development of the province of Los Ríos (the second most suitable agro-productive area at the national level) and in Ecuador; However, the distribution of these crops occurs without territorial planning according to the type of soil (Ministry of Agriculture, Livestock, Aquaculture and Fisheries, MAGAP, 2016; Salmoral et al., 2018). The main negative impact generated by inadequate land use planning is its degradation (Leng et al., 2020), so an orderly occupation of the territory is needed. For this, accurate information on current land cover is essential (Borràs et al., 2017).

With remote sensing, new arable hectares can be established, taking into account the behavior of the phenology of the species (Caparrós & Rodríguez-Galiano, 2020). Likewise, crop detection provides real information on the current use of the territory to propose and implement anticipatory measures (risk management) in the event of adverse climatic events (Giménez & Castaño, 2012). On the other hand, analysing the changes that are generated in the territory, estimating the eventual harvest and the classification of land use using high and medium resolution multispectral images, are also varied functionalities offered by remote sensing (Egea-Cobrero et al., 2018; Vélez & Álvarez, 2020).

In response to the need for information on land use and land cover, conventional methods have been used to classify multispectral images; However, with the passage of time, artificial intelligence and machine learning techniques have emerged (Cánovas-García et al., 2016). Among the alternate possibilities mentioned can be artificial neural networks, support vector machines, fuzzy theory, and decision trees (Mather & Tso, 2016). This research compares the performance of the traditional Maximum Probability (ML) method versus a decision tree-based technique, called Random Forest (RF), for the detection of bananas, cocoa and palm from Landsat-8 and Sentinel-2 multispectral images. Despite the fact that the results obtained with Random Forest are slightly higher, in different nuances, Maximum Likelihood was better. All of this was analyzed in the results and discussion of this research.

## 2. Materials and methods

### 2.1. Location

The study was conducted in the province of Los Ríos, Ecuador (cantons Baba, Vinces, Mocache and Palenque) (see Figure 1). The average temperature of the site is  $25^{\circ}\text{C}$ , and usually fluctuates between  $24^{\circ}\text{C}$  and  $27^{\circ}\text{C}$ . The area has a rainy season (from December to May) and a dry season; The maximum rainfall in the rainy season is 429 mm (February). At the study site, soils with fine, moderately coarse and fine textures predominate (GADPR, 2015).

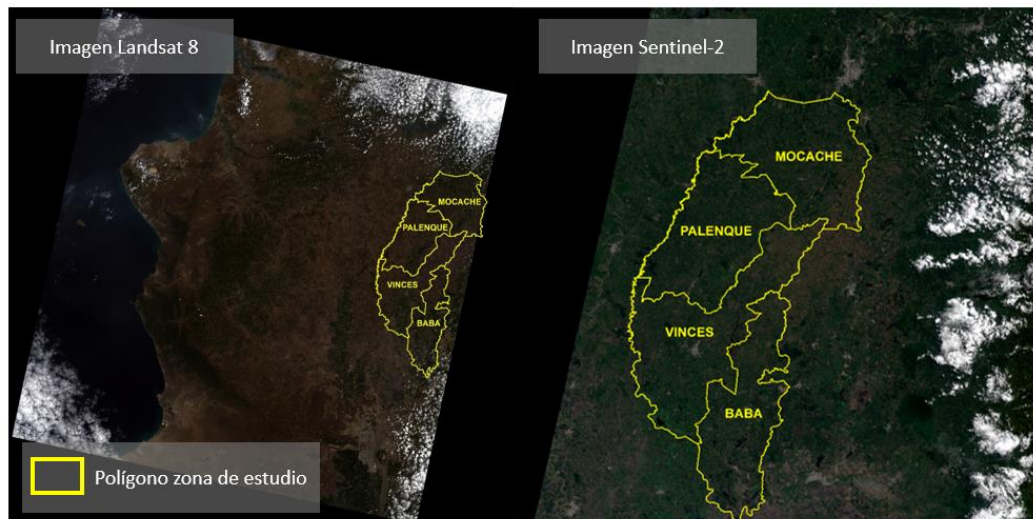


Figure 1. Spectral images used and study area

Source: USGS Science for a changing world

## 2.2. Download and pre-processing of multispectral images

The images were downloaded from the USGS Earth Explorer website. The Landsat-8 image is from the satellite program's Collection 1 Level 2 (with atmospheric correction) and was requested via email; The resolutions of its bands are 15 m (band 8), 30 m (bands 1, 2, 3, 4, 5, 6 and 7) and 100 m (bands 10 and 11). The Sentinel-2 image is of level 1C (no atmospheric correction) and was downloaded directly from the aforementioned website; the resolutions of its bands are 10 m (bands 2, 3, 4 and 8), 20 m (bands 5, 6, 7, 8A, 11 and 12) and 60 m (bands 1, 9 and 10) ( see Table 1).

Table 1. Information from the multispectral images used.

Image Information		
	Landsat-8	Sentinel-2
Spatial resolution (m)	15, 30 and 100	10, 20 and 60
Number of Bands	11	13
Date	27-11-2016	17-04-2018
Percentage of cloud cover	8.99%	4.32%
DATUM & Map Projection	WGS84	WGS84
UTM Zone	17 South	17 South
Other	It belongs to the 1 level 2 collection of the satellite program	Level 1C

Source: USGS Science for a changing world

All Sentinel-2 bands were weather-corrected in QGIS 3.16.8 software using the Semi-Automatic Classification Plugin of Congedo (2016) and used in the investigations of (Al-Masaodi & Al-Zubaidi, 2021; Belenok et al., 2021; Islam et al., 2021; Moraes Rocha et al., 2022). The atmospheric correction was applied because it allowed the conversion of the Sentinel-2 image from level 1C to level 2A (Bottom of Atmosphere), in order to obtain more accurate results in the eventual supervised classification (Sola et al., 2018).

### 2.3 Additional cropping of the study area

The polygon of the study area was cropped because the Landsat-8 and Sentinel-2 imagery did not cover the entire area. The area dispensed was 12.3876 km<sup>2</sup> (0.52% of the study area) (see Figure 2). After clipping, spectral indices were calculated (see 2.4).

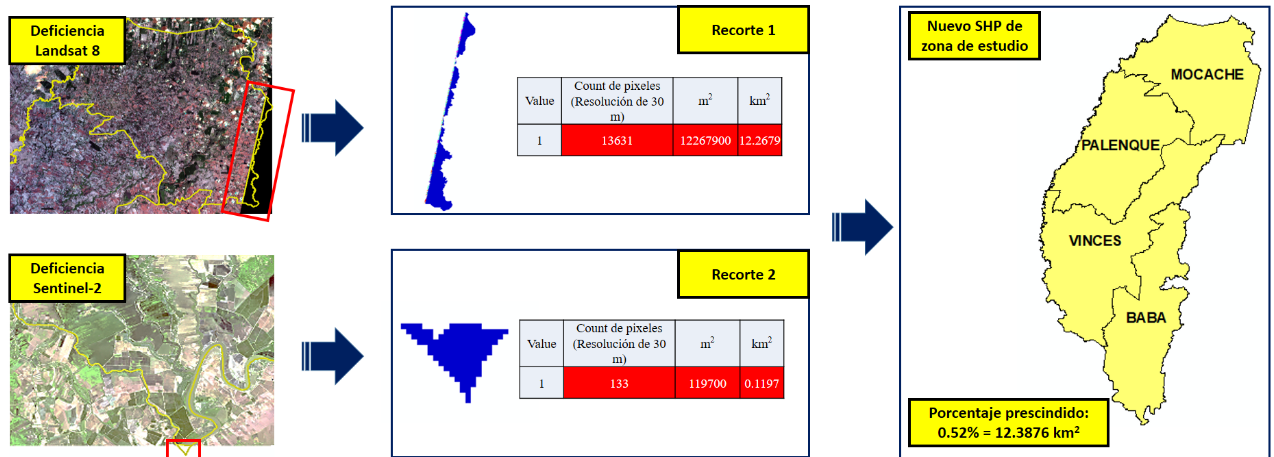


Figure 2. Crop of the additional study area by partial coverage of the satellite images.

### 2.4 Calculation of spectral indices

NDVI, GNDVI, MSI and GCI spectral indices were calculated in ENVI 5.3 software. The calculation of spectral indices and their stack (union of calculated indices) were essential for supervised classification. The equations for calculating the spectral indices are shown in Table 2.

Table 2. Equations for the calculation of spectral indices

#### Equations for Calculating Spectral Indices

$$NDVI = \frac{NIR - RED}{NIR + RED}$$

$$GNDVI = \frac{NIR - G}{NIR + G}$$

$$GCI = \frac{NIR}{G} - 1$$

$$MSI = \frac{MidIR}{NIR}$$

Source: (Tian et al., 2021; EOS, 2019; Welikhe et al., 2017; Sarker et al., 2021)

### 2.5 Creation of Regions of Interest (ROIs)

Initially, areas with banana, cocoa and palm crops, bodies of water, human settlements, without apparent vegetation and with other covers were identified. For identification, coordinates were taken in the aforementioned areas using Google Earth Pro; However, for cocoa cultivation, insitu coordinates were taken due to the complexity of identifying this coverage from software. Finally, the regions of interest were created in the ENVI 5.3 software (see Table 3); In addition, spectral separability values were calculated by applying the methodology described by (Howell & Yackel, 2014) ; This calculation made it possible to verify the quality of the ROIs created (which influence the results of the ranking).

Table 3. Number of pixels allocated per category in ROIs.

Category	Assigned Color	Number of pixels per category	
		Landsat-8	Sentinel-2
Areas with banana cultivation		387	1099
Areas with cocoa crops		200	481
Areas with palm plantations		219	1384
Areas with bodies of water		247	1344
Areas with no apparent vegetation		963	1910
Areas with human settlements		716	1263
Areas with other coverages		609	10869
Clouds		1481	Not Considered

### 2.6 Supervised classification

Supervised classification with ML (conventional method in remote sensing) was performed in ENVI 5.3; It uses quadratic or linear discrimination functions and the classes (ROIs) are assigned according to the maximum probability of the pixel according to the regions of interest created (Ha et al., 2020). On the other hand, QGIS was used for the classification with Random Forest, and the Dzetsaka plugins created by Karasiak (2019) and used in the (Ju & Bohrer, 2022; Palafox-Juárez et al., 2021; Santarsiero et al., 2022; Sejati et al., 2020).

### 2.7 Validation of results

To check the results, random coordinates were taken in Google Earth from all categories, except for "Areas with cocoa crops" (again insitu coordinates were taken). With these new coordinates, other ROIs were created on the calculated index stacks (see 2.4)

Next, a confusion matrix was made, which is a double-entry table, where each category represents a row and a column within the table. The double entry allows you to compare the actual values with the results of the post-classification with different ROIs and raise; Therefore, the diagonal of the matrix indicates the pixels that match, while the other values (vertical) indicate the pixels that were confused with other categories (classification error) (Borràs et al., 2017).

The Confusion Matrix of (John, 1986), is a fairly common methodology in remote sensing and has been cited in different studies around the world, including those of (Borràs et al., 2017; Pinto-Hidalgo & Silva-Centeno, 2022; Rouibah & Belabbas, 2020; Valbuena et al., 2016).

In the same way, the Kappa coefficient proposed by Cohen (1960) and used in the investigations of (Borràs et al., 2017; Rouibah & Belabbas, 2020; Valbuena et al., 2016). The result of the calculation (performed in ENVI 5.3) indicates the level of accuracy or adjustment of the classification. Between 0.01 and 0.20 represents a slight agreement, between 0.21 and 0.40 represents an acceptable agreement, between 0.41 and 0.60 a moderate agreement, between 0.61 and 0.80 a considerable agreement, and between 0.81 and 1 a near perfect agreement (Cohen, 1960).

### 3. Results

#### 3.1 Calculation of spectral indices

The NDVI of Sentinel-2 (E) obtained a greater presence of dense vegetation compared to the NDVI of Landsat-8 (A). Similarly, the values of GNDVI (photosynthetic activity) and GCI (chlorophyll content) of Sentinel-2 (F and H) were higher than those reported by the same indices for Landsat-8 (B and D). In contrast, the Landsat-8 (C) MSI (water stress) index had higher values than those reported by Sentinel-2 (G). These obvious differences are due to the seasonal differences between the two images; the Landsat-8 image corresponds to the dry season, while the Sentinel-2 image belongs to the rainy season. Therefore, it is evident that in the Sentinel-2 image there will be more dense vegetation, which results in higher photosynthetic activity and chlorophyll levels in the leaves, as well as less water stress (see Figure 3).

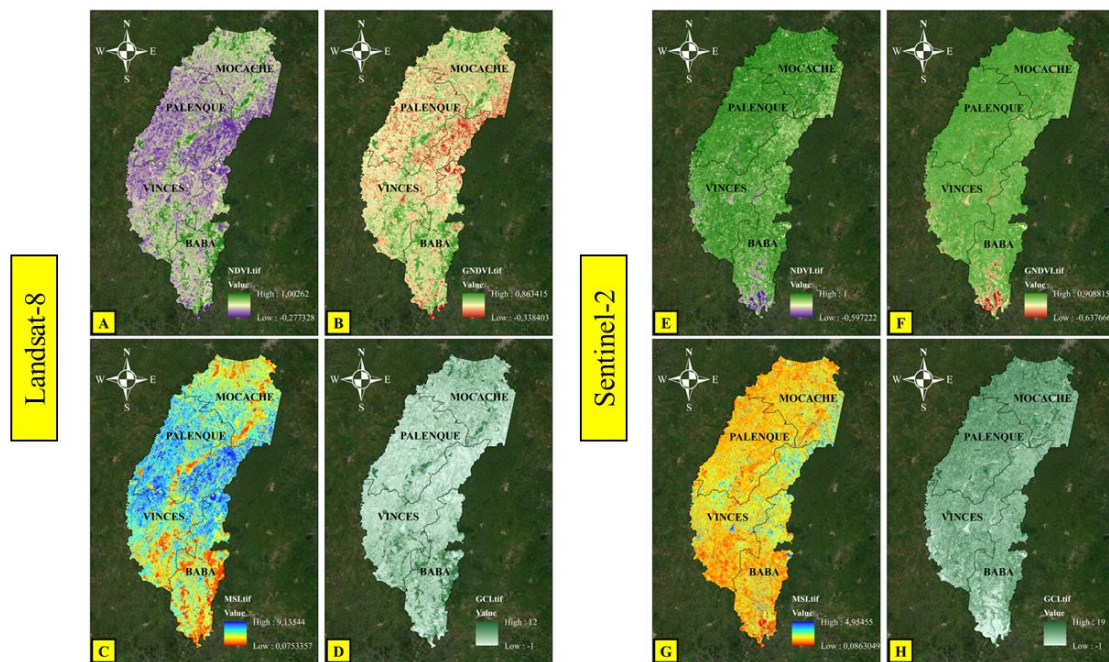


Figure 3. Landsat-8 and Sentinel-2 spectral indices representation: A(NDVI Landsat-8) – B(GNDVI Landsat-8) – C(MSI Landsat-8) – D(GCI Landsat-8) – E(NDVI Sentinel-2) – F(GNDVI Sentinel-2) – G(MSI Sentinel-2) – H(GCI Sentinel-2).

#### 3.2 Spectral separability

The spectral separability of the ROIs of the Sentinel-2 (B) index stack was better than the spectral separability obtained for Landsat-8 (A); the improvement of Sentinel-2 is due to better spatial resolution in its bands. The spectral separability values between the categories "Areas with cocoa crops" and "Areas with other covers" were the lowest for both Landsat-8 (1.47) and Sentinel-2 (1.90). The low spectral separability mentioned is due to the fact that it was not possible to identify large areas of unique areas with cocoa crops (it is common for it not to be planted in large areas or always together with other types of crops), making it difficult to create good ROIs for this category, especially in Landsat-8 (lower spatial resolution). However, for Landsat-8, 26 of the 28 spectral separability values calculated ranged from 1.86 to 2 (very high separability); In the same vein, for the Sentinel-2 Stack, 20 of the 21 calculated values fluctuated between 1.94 and 2 (see Figure 4).

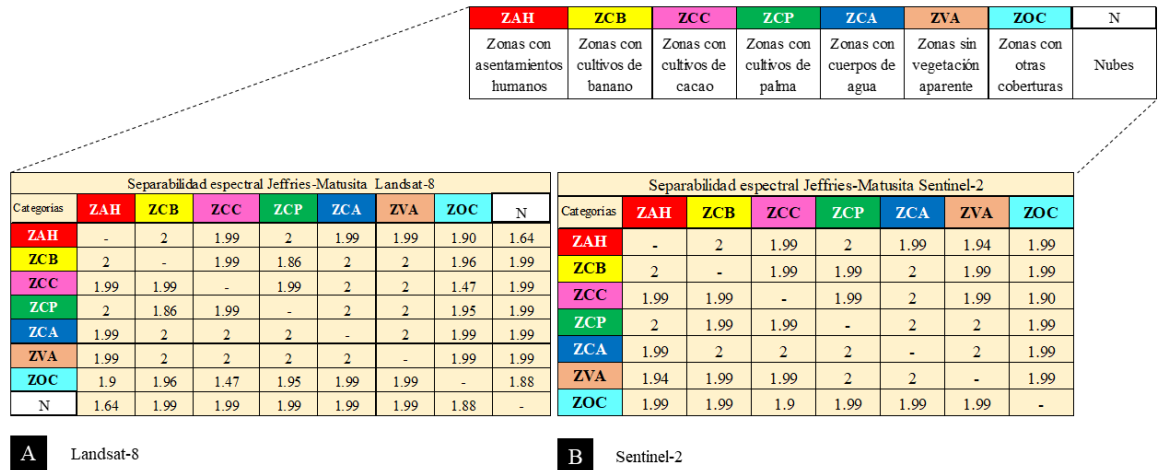


Figure 4. Jeffries-Matusita spectral separability of calculated index stack ROIs: A: Landsat-8 and B: Sentinel-2

### 3.2 Supervised classification

#### 3.2.1 Landsat-8 classification

2609249 Pixels with spatial resolution of 30 m x 30 m were identified in both the Landsat-8 classification with ML (A) and RF (B). Both ML (1512.96 km<sup>2</sup>) and RF (1242.09 km<sup>2</sup>) detected that the category "Zones with other coverage" predominates in the occupation of land use in the study area. Similarly, in both classifications, the category with the lowest territorial occupation was "Areas with bodies of water", with 21.21 km<sup>2</sup> using ML and 14.91 km<sup>2</sup> using RF. In relation to the detection objectives (areas with banana, cocoa and palm crops), in both classifications cocoa cultivation had the largest territorial extension (208.71 km<sup>2</sup> with ML and 222.68 km<sup>2</sup> with RF), followed by banana cultivation (74.83 km<sup>2</sup> with ML and 118.52 km<sup>2</sup> with RF) and palm cultivation (24.19 km<sup>2</sup> with ML and 15.30 km<sup>2</sup> with RF) (see Figure 5).

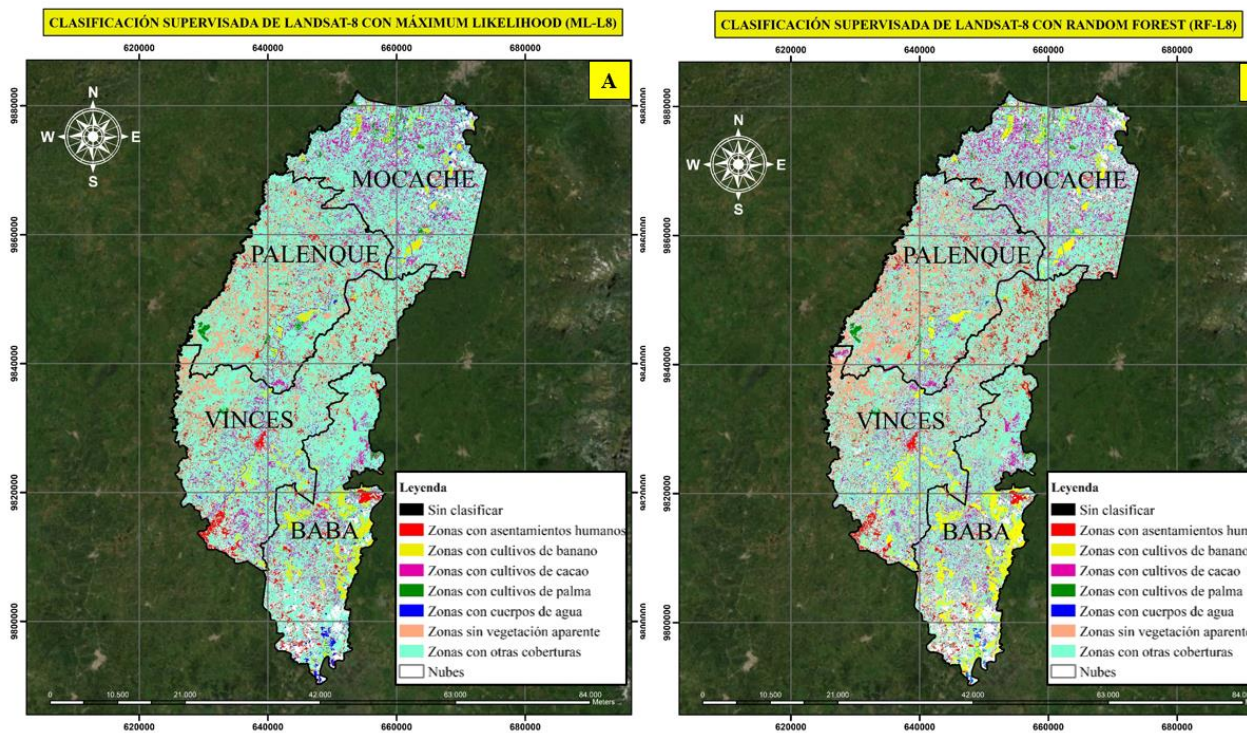


Figure 5. Supervised Landsat-8 classification. A: ML-L8 and B: RF-L8

### 3.2.1 Sentinel-2 classification

23483177 Pixels with spatial resolution of 10 m x 10 m were identified in both the Sentinel-2 classification with ML (A) and RF (B). As in the Landsat-8 classifications, for Sentinel-2, both with ML (1091.29 km<sup>2</sup>) and RF (1631.51 km<sup>2</sup>), it was detected that the category "Areas with other coverages" predominates in the land use occupation of the area. However, ML detected that the category with the smallest area was "Areas with palm plantations" with 31.23 km<sup>2</sup>, while RF "Areas with banana crops" with 26.55 km<sup>2</sup>; all totally different from what was detected by the same classifiers for Landsat-8. In addition, it should be noted that ML detected 500.30 km<sup>2</sup> of cocoa and 34.97 km<sup>2</sup> of bananas; in the same sense, RF detected 26.68 km<sup>2</sup> of palm and 130.96 km<sup>2</sup> of cocoa (see Figure 6).

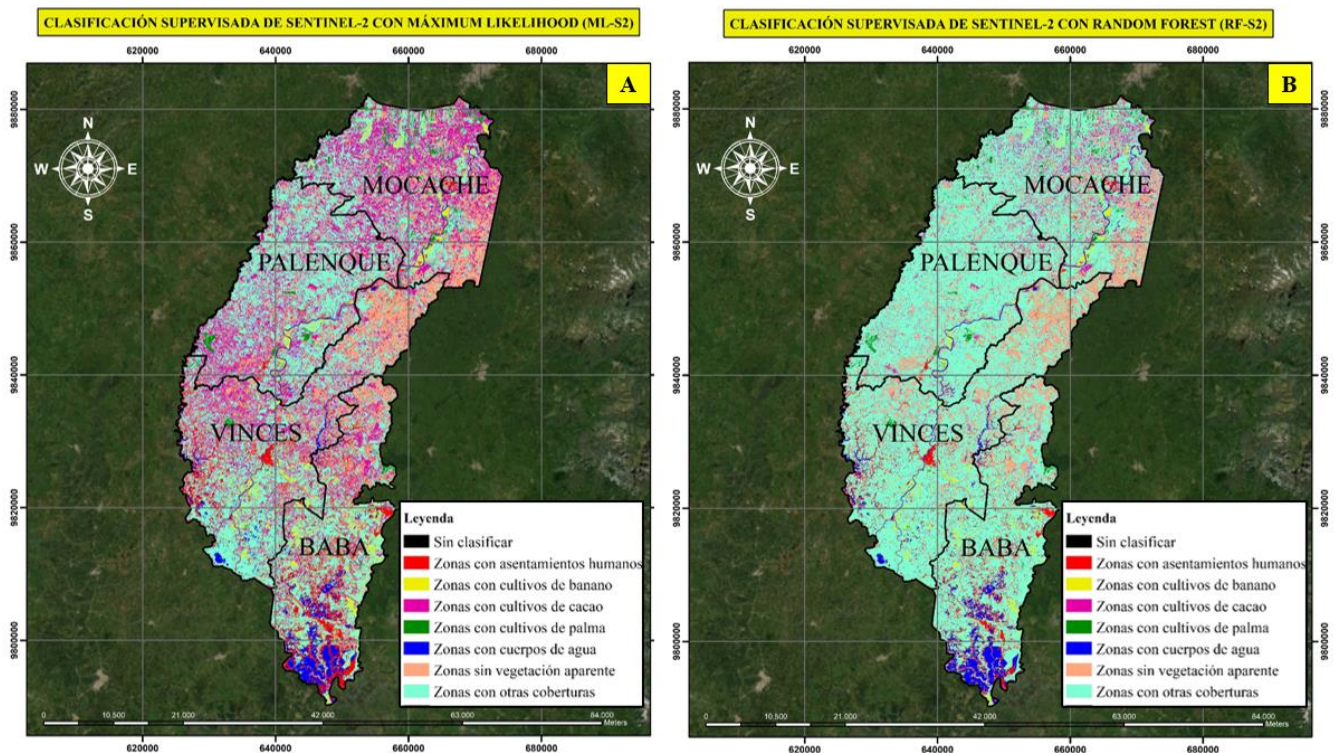


Figure 6. Supervised classification of Sentinel-2. A: ML-S2 and B: RF-S2

## 3.3 Validation of results

### 3.3.1 Confusion matrices

The most accurate classification was Sentinel-2 with Random Forest (89%) and the least accurate was Sentinel-2 with Maximum Likelihood (76%). In the rankings, the percentages of agreement/accuracy for areas with banana, cocoa and palm crops ranged from 33.85% (the lowest percentage) to 98.63% (the highest percentage) (see Figure 7).

According to Figure 7, cocoa could not be accurately detected with any classifier (ML-L8: 50%, RF-L8: 41.67%, RF-S2: 33.85% and ML-S2: 54.36%). On the other hand, areas with palm (values above 96.17% with ML-L8, ML-S2 and RF-L8) and banana (values above 96.58% with ML-L8 and RF-L8) could be detected with a fair degree of accuracy. The classification with the best detection accuracy for bananas, cocoa, and palm was ML-L8 (98.63%, 50%, and 96.30%, respectively) and the lowest accurate was RF-S2 (agreement/accuracy values below 72.84%) (see Figure 7).

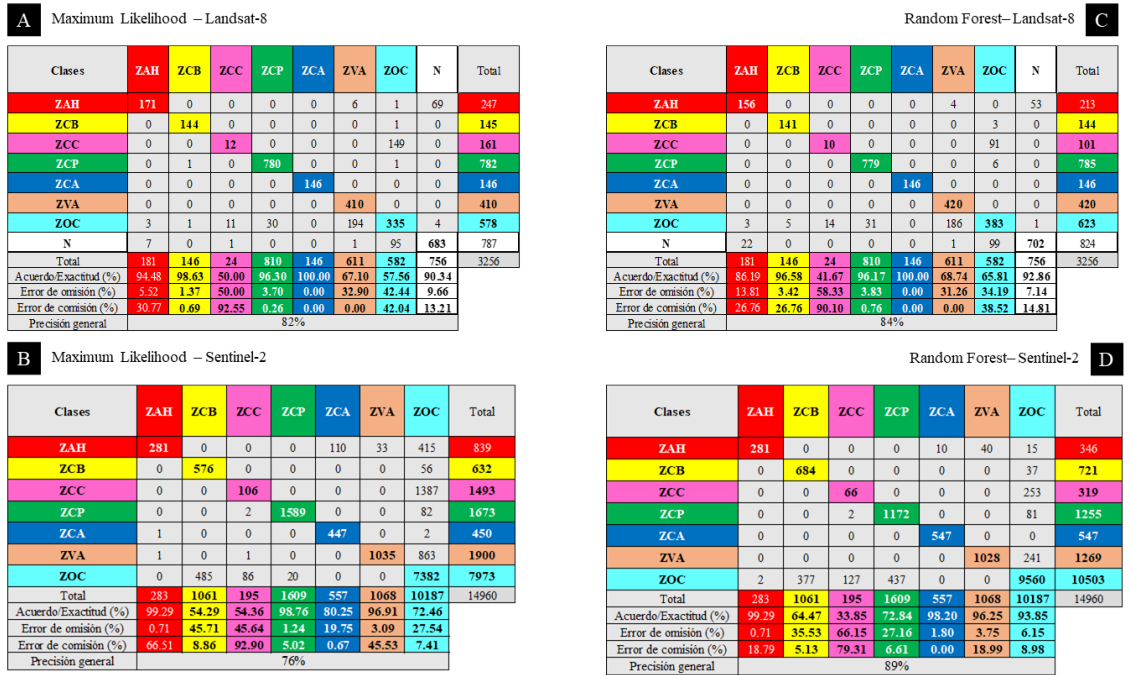


Figure 7. Confusion matrices: A: ML-L8, B: ML-S2, C: RF-L8 and D: RF-S2.

### 3.3.2 Kappa coefficients

According to the Kappa coefficient, all the rankings were considerable. The most accurate was Landsat-8 with Random Forest (0.80) and the least accurate was Sentinel-2 with Maximum Likelihood (0.61) (same as in Figure 7). The most accurate classifications were obtained with Landsat-8; however, Random Forest with Sentinel-2 obtained a fairly close accuracy (0.78) (see Table 4).

Table 4. Kappa coefficients for classifications made with Maximum Likelihood and Random Forest.

Classification	Kappa coefficient	Precision
Maximum Likelihood – Landsat-8	0.79	Considerable
Maximum Likelihood – Sentinel-2	0.61	Considerable
Random Forest – Landsat-8	0.80	Considerable
Random Forest – Sentinel-2	0.78	Considerable

## 4. Discussion

The Maximum Likelihood method has been one of the most widely used for decades for the classification of multispectral images; however, new AI-based methods such as Random Forest have emerged (Cánovas-García et al., 2016; Mather & Tso, 2016). This includes the need to check the accuracy of these new classification methods. In addition, in the province of Los Ríos, where agricultural production is transcendental in socioeconomic conditions (Ministry of Agriculture, Livestock, Aquaculture and Fisheries, 2016), up-to-date mapping of the distribution of the most important crops is essential (Borràs et al., 2017), as the maps offered by public government entities are often outdated and it is common for agricultural areas to be lumped into macro categories.

For the detection of different crops, it is common to use spectral indices of vegetation as it increases the chances of obtaining an accurate classification (Denis Ávila et al., 2020; Fei et al., 2011). Different vegetation indices have been tested in several studies, such as

NDVI and the Soil-Adjusted Vegetation Index (SAVI), among others (Munyati, 2022). Precisely, NDVI is one of the most widely used indices; For example, it has been used for the estimation of the mangrove leaf area index (Guo et al., 2021), to determine the ecological dynamics of forest vegetation (Právělie et al., 2022), among many other studies around the world. In this study, NDVI, GNDVI, GCI and MSI were used to form a stack of indexes for each image and on these to create the ROIs and generate the rankings.

Although, with other vegetation indices and other types of pre-processing, Maximum Likelihood and Random Forest have also obtained accurate results (Ali et al., 2018; Axelsson et al., 2021; Ge et al., 2020; Shivakumar & Rajashekararadhya, 2018), the classifications made in this research, obtained considerable accuracy according to the Kappa coefficient, with overall accuracy percentages between 82% and 89% (according to the confounding matrix). It should be noted that, with better and more training data, the accuracies could have ranged between 95% and 99% (Borràs et al., 2017; Sharma et al., 2017).

While the overall accuracy of the classifications fluctuates between 82% and 89%, the detection accuracy for two (banana and palm) of the three main detection targets was excellent (above 96%). In contrast, cocoa was not accurately detected in any classification (agreement/accuracy values below 55%). This was due to the low spectral separability of areas with cocoa crops with the category "Zones with other covers". This occurred because no extensive coverage of cocoa crops was identified in the area, since it is generally not planted in large areas or is planted next to others. Consequently, it is possible to affirm according to (E. D. Chaves et al., 2020; Weiss et al., 2020) that the detection of this crop was not accurate, since the lack of field samples to train the classifiers was the great limitation.

Generally, Maximum Likelihood detects areas with agricultural crops very accurately in Landsat-8 and Sentinel-2 imagery, as does Random Forest (Ali et al., 2018; Borràs et al., 2017; Campos-Taberner et al., 2020; Ge et al., 2020; Pareeth et al., 2019; Santiago Bazán et al., 2021; Song et al., 2021). In this case, the best classification for the detection of bananas, cocoa and palm (together) was that of Landsat-8 using Maximum Likelihood, while the least accurate was that of Sentinel-2 using Random Forest; however, RF-S2 in overall accuracy (encompassing water, urban use, without vegetation and other coverage) was the most accurate. The low accuracy of RF-S2 for the detection of these three cultures is due to two main reasons. The first reason was due to the season of the Sentinel-2 image (rainy season), which has a significant influence on the (Gomariz-Castillo et al., 2017; Rodríguez-Valero & Alonso-Sarria, 2019). The second reason was due to the lack of field data for cocoa crops (as previously mentioned) (E. D. Chaves et al., 2020; Weiss et al., 2020).

## 5. Conclusion

The results allow us to conclude that Random Forest was the method with the highest overall accuracy, although the difference using Maximum Likelihood was not significant. However, for the detection of bananas, cocoa and palm, the best method was Maximum Likelihood with Landsat-8 imagery (lower spatial resolution). It is suggested that, in future comparative studies, a greater number of insitu coordinates be taken for cocoa cultivation; In addition, to use Sentinel-2 images in the dry season, because it is presumed that the low accuracy (especially with RF-S2) in the detection of the target crops was due to the season of image acquisition (rainy season).

## Thanks

This research has been carried out as part of the 8th FOCICYT-UTEQ project "Comparative analysis of artificial intelligence algorithms applied for detection and evaluation of the state of cocoa, palm and banana crops in the province of Los Ríos from the images of the Landsat-8 and Sentinel-2 satellites" funded by the State Technical University of Quevedo, Quevedo, Ecuador.

## References

- Al-Masaodi, H. J. O., & Al-Zubaidi, H. A. M. (2021). Spatial-temporal changes of land surface temperature and land cover over Babylon Governorate, Iraq. *Materials Today: Proceedings*. <https://doi.org/10.1016/j.matpr.2021.05.179>
- Ali, M. Z., Qazi, W., & Aslam, N. (2018). A comparative study of ALOS-2 PALSAR and landsat-8 imagery for land cover classification using maximum likelihood classifier. *The Egyptian Journal of Remote Sensing and Space Science*, 21, S29–S35. <https://doi.org/10.1016/j.ejrs.2018.03.003>
- Axelsson, A., Lindberg, E., Reese, H., & Olsson, H. (2021). Tree species classification using Sentinel-2 imagery and Bayesian inference. *International Journal of Applied Earth Observation and Geoinformation*, 100. <https://doi.org/10.1016/j.jag.2021.102318>
- Belenok, V., Noszczyk, T., Hebyn-Baidy, L., & Kryachok, S. (2021). Investigating anthropogenically transformed landscapes with remote sensing. *Remote Sensing Applications: Society and Environment*, 24. <https://doi.org/10.1016/j.rsase.2021.100635>
- Borràs, J., Delegido, J., Pezzola, A., Pereira, M., Morassi, G., & Camps-Valls, G. (2017). Land use classification from Sentinel-2 imagery. *Journal of Remote Sensing*, 48, 55. <https://doi.org/10.4995/raet.2017.7133>
- Campos-Taberner, M., García-Haro, F. J., Martínez, B., & Gilabert, M. A. (2020). Deep learning for agricultural land use classification with Sentinel-2. *Journal of Remote Sensing*, 56, 35. <https://doi.org/10.4995/raet.2020.13337>
- Cánovas-García, F., Alonso, F., & Castillo, F. (2016). Modification of the Random Forest algorithm for use in remote sensing image classification (pp. 359–368).
- Caparros, J. A., & Rodríguez-Galiano, V. (2020). Estimation of vegetation phenology from satellite images: the case of the Iberian Peninsula and the Balearic Islands (2001-2017). *Journal of Remote Sensing*, 57, 25–36. <https://doi.org/10.4995/raet.2020.13632>
- Cerda Lorca, J., & Villarroel, L. (2008). Evaluation of inter-observer concordance in paediatric research: Kappa coefficient. *Chilean Journal of Pediatrics*, 79(1), 54–58. <https://doi.org/10.4067/s0370-41062008000100008>
- Cohen, J. (1960). A Coefficient of Agreement for Nominal Scales. *Educational and Psychological Measurement*, 20(1), 37–46. <https://doi.org/10.1177/001316446002000104>
- Congedo, L. (2021). Semi-Automatic Classification Plugin: A Python tool for the download and processing of remote sensing images in QGIS. *Journal of Open Source Software*, 6(64), 3172. <https://doi.org/10.21105/joss.03172>
- Denis Ávila, D., Curbelo, E. A., Madrigal-Roca, L. J., & Pérez-Lanyau, R. D. (2020). Spatio-temporal variation of the spectral response in mangroves in Havana, Cuba, evaluated with remote sensing. *Journal of Tropical Biology*, 68(1), 321–335.
- E. D. Chaves, M., C. A. Picoli, M., & D. Sanches, I. (2020). Recent Applications of Landsat 8/OLI and Sentinel-2/MSI for Land Use and Land Cover Mapping: A Systematic Review. *Remote Sensing*, 12(18), 3062. <https://doi.org/10.3390/rs12183062>
- Egea-Cobrero, V., Rodríguez, V., Sánchez-Rodríguez, E., & García-Pérez, M. A. (2018). Estimation of the wheat harvest in Andalusia using time series of the MERIS Terrestrial Chlorophyll Index (TCIM). *Journal of Remote Sensing*, 51, 99–112. <https://doi.org/10.4995/raet.2018.8891>

- EOS. (2019). 6 Spectral Indexes To Make Vegetation Analysis Complete. Agriculture. <https://eos.com/blog/6-spectral-indexes-on-top-of-ndvi-to-make-your-vegetation-analysis-complete/>
- Fei, S. X., Shan, C. H., & Hua, G. Z. (2011). Remote Sensing of Mangrove Wetlands Identification. *Procedia Environmental Sciences*, 10, 2287–2293. <https://doi.org/10.1016/j.proenv.2011.09.357>
- GADPR. (2015). Development and Land Use Plan 2015-2019 (p. 300). Decentralized Autonomous Provincial Government of Los Ríos.
- Gama-Rodrigues, A., Müller, M. W., Gama-Rodrigues, E., & Mendes, F. A. (2021). Cacao-based agroforestry systems in the Atlantic Forest and Amazon Biomes: An ecoregional analysis of land use. *Agricultural Systems*, 194. <https://doi.org/10.1016/j.agsy.2021.103270>
- Ge, G., Shi, Z., Zhu, Y., Yang, X., & Hao, Y. (2020). Land use/cover classification in an arid desert-oasis mosaic landscape of China using remote sensed imagery: Performance assessment of four machine learning algorithms. *Global Ecology and Conservation*, 22. <https://doi.org/10.1016/j.gecco.2020.e00971>
- Giménez, A., & Castaño, J. (2012). Estimation of areas occupied by winter crops in Uruguay using remote sensing. *Mexican Journal of Agricultural Sciences*, 3(2), 391–396.
- Gomariz-Castillo, F., Alonso-Sarría, F., & Cánovas-García, F. (2017). Improving Classification Accuracy of Multi-Temporal Landsat Images by Assessing the Use of Different Algorithms, Textural and Ancillary Information for a Mediterranean Semiarid Area from 2000 to 2015. *Remote Sensing*, 9(10), 1058. <https://doi.org/10.3390/rs9101058>
- Guo, X., Wang, M., Jia, M., & Wang, W. (2021). Estimating mangrove leaf area index based on red-edge vegetation indices: A comparison among UAV, WorldView-2 and Sentinel-2 imagery. *International Journal of Applied Earth Observation and Geoinformation*, 103, 102493. <https://doi.org/10.1016/j.jag.2021.102493>
- Ha, N. T., Manley-Harris, M., Pham, T. D., & Hawes, I. (2020). A Comparative Assessment of Ensemble-Based Machine Learning and Maximum Likelihood Methods for Mapping Seagrass Using Sentinel-2 Imagery in Tauranga Harbor, New Zealand. *Remote Sensing*, 12(3), 355. <https://doi.org/10.3390/rs12030355>
- Howell, S., & Yackel, J. (2014). The Jeffries–Matusita distance for the case of complex Wishart distribution as a separability criterion for fully polarimetric SAR data. *International Journal of Remote Sensing*, 35(19), 6859–6873. <https://doi.org/10.1080/01431161.2014.960614>
- Islam, M. R. three decade assessment of forest cover changes in N. dwip national park using remote sensing and G., Khan, M. N. I., Khan, M. Z., & Roy, B. (2021). A three decade assessment of forest cover changes in Nijhum dwip national park using remote sensing and GIS. *Environmental Challenges*, 4. <https://doi.org/10.1016/j.envc.2021.100162>
- John, J. (1986). *Introductory Digital Image Processing: A Remote Sensing Perspective*. Prentice-Hall.
- Ju, Y., & Bohrer, G. (2022). Classification of Wetland Vegetation Based on NDVI Time Series from the HLS Dataset. *Remote Sensing*, 14(9), 2107. <https://doi.org/10.3390/rs14092107>
- Karasiak, N. (2019). lenepkade/dzetsaka: Fix bug in processing provider with vector files (v3.5.1). In Zenodo. Zenodo. <https://doi.org/10.5281/zenodo.3463523>
- Leng, X., Feng, X., & Fu, B. (2020). Driving forces of agricultural expansion and land degradation indicated by Vegetation Continuous Fields (VCF) data in drylands from 2000 to 2015. *Global Ecology and Conservation*, 23, e01087. <https://doi.org/10.1016/j.gecco.2020.e01087>
- Mather, P., & Tso, B. (2016). *Classification Methods for Remotely Sensed Data (Second)*. CRC Press. <https://doi.org/10.1201/9781420090741>
- MCPEC, MEER, & INP. (2014). *Bioenergetic Atlas of Ecuador*.
- Ministry of Agriculture, Livestock, Aquaculture and Fisheries, MAGAP. (2016). Ecuadorian agricultural policy. Towards sustainable rural territorial development 2015-2025. In Ministry of Agriculture and Livestock. <http://www.fao.org/3/i5778s/i5778s.pdf>

- Moraes Rocha, B., Ueslei da Fonseca, A., Pedrini, H., & Soares, F. (2022). Automatic detection and evaluation of sugarcane planting rows in aerial images. *Information Processing in Agriculture*. <https://doi.org/10.1016/j.inpa.2022.04.003>
- Munyati, C. (2022). Detecting the distribution of grass aboveground biomass on a rangeland using Sentinel-2 MSI vegetation indices. *Advances in Space Research*, 69(2), 1130–1145. <https://doi.org/10.1016/j.asr.2021.10.048>
- Osvaldo Bardoniano, M. (2014). Ecuador: Recent Economic Developments and Outlook. *Economía Informa*, 385, 100–108. [https://doi.org/10.1016/S0185-0849\(14\)70424-4](https://doi.org/10.1016/S0185-0849(14)70424-4)
- Palafox-Juárez, E. B., López-Martínez, J. O., Hernández-Stefanoni, J. L., & Hernández-Núñez, H. (2021). Impact of Urban Land-Cover Changes on the Spatial-Temporal Land Surface Temperature in a Tropical City of Mexico. *ISPRS International Journal of Geo-Information*, 10(2), 76. <https://doi.org/10.3390/ijgi10020076>
- Pareeth, S., Karimi, P., Shafiei, M., & De Fraiture, C. (2019). Mapping Agricultural Landuse Patterns from Time Series of Landsat 8 Using Random Forest Based Hierarchical Approach. *Remote Sensing*, 11(5), 601. <https://doi.org/10.3390/rs11050601>
- Pinto-Hidalgo, J. J., & Silva-Centeno, J. A. (2022). AmazonCRIME: a Geospatial Artificial Intelligence dataset and benchmark for the classification of potential areas linked to Transnational Environmental Crimes in the Amazon Rainforest. *Journal of Remote Sensing*, 59, 1–21. <https://doi.org/10.4995/raet.2022.15710>
- Prăvălie, R., Sîrodoev, I., Nita, I.-A., Patriche, C., Dumitraşcu, M., Roşca, B., Tişcovschi, A., Bandoc, G., Săvulescu, I., Mănoiu, V., & Birsan, M.-V. (2022). NDVI-based ecological dynamics of forest vegetation and its relationship to climate change in Romania during 1987–2018. *Ecological Indicators*, 136, 108629. <https://doi.org/10.1016/j.ecolind.2022.108629>
- Rodríguez-Valero, M. I., & Alonso-Sarria, F. (2019). Classification of Landsat-8 images in the Segura River Basin District. *Journal of Remote Sensing*, 53, 33–44. <https://doi.org/10.4995/raet.2019.11016>
- Rouibah, K., & Belabbas, M. (2020). Applying Multi-Index approach from Sentinel-2 Imagery to Extract Urban Area in dry season (Semi-Arid Land in North East Algeria). *Journal of Remote Sensing*, 56, 89–101. <https://doi.org/10.4995/raet.2020.13787>
- Salmoral, G., Khatun, K., Llive, F., & Lopez, C. M. (2018). Agricultural development in Ecuador: A compromise between water and food security? *Journal of Cleaner Production*, 202, 779–791. <https://doi.org/10.1016/j.jclepro.2018.07.308>
- Sánchez Castañeda, J. (2017). Organic agricultural products market in Colombia. *Sum of Business*, 8, 156–163. <https://doi.org/10.1016/j.sumneg.2017.10.001>
- Santarsiero, V., Nolè, G., Lanorte, A., Tucci, B., Cillis, G., & Murgante, B. (2022). Remote Sensing and Spatial Analysis for Land-Take Assessment in Basilicata Region (Southern Italy). *Remote Sensing*, 14(7), 1692. <https://doi.org/10.3390/rs14071692>
- Santiago Bazán, F., Mallqui Meza, H., & Ríos Recra, R. (2021). Mapping of vegetation cover in the Quillcay sub-basin (Ancash – Peru) with the Decision Tree classifier. *Santiagoino Contribution*, 14(1), 78–91. <https://doi.org/10.32911/as.2021.v14.n1.761>
- Sarker, M. N. U., Ulfat, F., Siddique, M. Z. A., & Farah, T. (2021). Unsupervised Learning-based Vegetation change detection with Landsat 8 data. *IEEE Xplore*, 368–372. <https://doi.org/10.1109/ICAIS50930.2021.9395869>
- Sejati, A. W., Buchori, I., Kurniawati, S., Brana, Y. C., & Fariha, T. I. (2020). Quantifying the impact of industrialization on blue carbon storage in the coastal area of Metropolitan Semarang, Indonesia. *Applied Geography*, 124. <https://doi.org/10.1016/j.apgeog.2020.102319>
- Sharma, R., Hara, K., & Tateishi, R. (2017). High-Resolution Vegetation Mapping in Japan by Combining Sentinel-2 and Landsat 8 Based Multi-Temporal Datasets through Machine Learning and Cross-Validation Approach. *Land*, 6(3), 50. <https://doi.org/10.3390/land6030050>

- Shivakumar, B. R., & Rajashekararadhya, S. V. (2018). Investigation on land cover mapping capability of maximum likelihood classifier: A case study on North Canara, India. *Computer Science*, 143, 579–586. <https://doi.org/10.1016/j.procs.2018.10.434>
- SIPA. (2021). Main agricultural products. Public Agricultural Production System. <http://sipa.agricultura.gob.ec/index.php>
- Sola, I., García-Martín, A., Sandonís-Pozo, L., Álvarez-Mozos, J., Pérez-Cabello, F., González-Audícana, M., & Montorio Llovería, R. (2018). Assessment of atmospheric correction methods for Sentinel-2 images in Mediterranean landscapes. *International Journal of Applied Earth Observation and Geoinformation*, 73, 63–76. <https://doi.org/10.1016/j.jag.2018.05.020>
- Song, X.-P., Huang, W., Hansen, M. C., & Potapov, P. (2021). An evaluation of Landsat, Sentinel-2, Sentinel-1 and MODIS data for crop type mapping. *Science of Remote Sensing*, 3, 100018. <https://doi.org/10.1016/j.srs.2021.100018>
- Tian, X., Zhang, M., Yang, C., & Ma, J. (2021). FusionNDVI: A Computational Fusion Approach for High-Resolution Normalized Difference Vegetation Index. *IEEE Transactions on Geoscience and Remote Sensing*, 59(6), 5258–5271. <https://doi.org/10.1109/TGRS.2020.3014698>
- USGS. (n.d.). Earth Explorer. <https://earthexplorer.usgs.gov/>
- Valbuena, R., Maltamo, M., & Packalen, P. (2016). Classification of forest development stages from national low-density lidar datasets: a comparison of machine learning methods. *Journal of Remote Sensing*, 45, 15. <https://doi.org/10.4995/raet.2016.4029>
- Vélez, D. A., & Álvarez, J. (2020). Classification of land uses and land cover and analysis of changes in the surroundings of the Churute Mangrove Ecological Reserve (Ecuador) using a series of Sentinel-1 images. *Journal of Remote Sensing*, 56, 131–146. <https://doi.org/10.4995/raet.2020.14099>
- Weiss, M., Jacob, F., & Duveiller, G. (2020). Remote sensing for agricultural applications: A meta-review. *Remote Sensing of Environment*, 236, 111402. <https://doi.org/10.1016/j.rse.2019.111402>
- Welikhe, P., Quansah, J. E., Fall, S., & McElhenney, W. (2017). Estimation of Soil Moisture Percentage Using LANDSAT-based Moisture Stress Index. *Journal of Remote Sensing & GIS*, 06(01). <https://doi.org/10.4172/2469-4134.1000200>